CORTICAL BONE FRACTURE

R. O. RITCHIE
University of California
Berkeley, California
J. H. KINNEY
Lawrence Livermore National Laboratory
Livermore, California
J. J. KRUZIC
Oregon State University
Corvallis, Oregon
R. K. NALLA
Intel Corporation
Chandler, Arizona

1. INTRODUCTION

The structural integrity of "hard" mineralized tissues such as bone is of great importance, especially because bone is the primary structural component of the body, serving as a protective load-bearing skeletal framework. As a structural material, bone is unique when compared with other engineering materials because of its well-known capacity for self-repair and adaptation to changes in mechanical usage patterns (e.g., see Refs. 1–5). Unfortunately, bone mass decreases with aging; furthermore, elevation in bone turnover, concurrent with menopause in aging women, can lead to osteoporosis, a condition of low bone mass associated with an increased risk of fracture. However, low bone mass is not the sole reason why bone becomes more prone to fracture with age; indeed, the recent realization that bone mineral density alone cannot explain the therapeutic benefits of antiresorptive agents in treating osteoporosis (6,7) has re-emphasized the necessity for understanding how other factors control bone fracture. Much of this renewed emphasis is currently being focused on "bone quality," where quality is a term used to describe some, as yet not clearly known, characteristics of the tissue that influence a broad spectrum of mechanical properties such as elastic modulus, strength, and toughness. Although there have been many studies on how such mechanical properties vary with age, disease, and changes in microstructure (8–30), there still remains much to be determined about how variations within the hierarchical microstructure of bone alter the fracture properties.

The underlying microstructure of cortical bone is quite complex. The basic building blocks, namely an organic matrix (90% type-I collagen, 10% amorphous ground substance) and mineral phase (calcium phosphate-based hydroxyapatite), are similar for all collagen-based mineralized tissues, although the ratio of these components and the complexity of the structures they form varies with the function of the particular tissue and the organ it forms. The composition and the structure of bone are not invariant; they vary with factors such as skeletal site, age, sex, physiological function, and mechanical loading, making bone a very heterogeneous structure. On average, however, the organic/mineral ratio in human cortical bone is roughly 1:1 by volume and 1:3 by weight.

The hierarchical structure of bone (14,16,31) can be considered at several dimensional scales (14). At nanoscale dimensions, bone is composed of type-I mineralized collagen fibers (up to 15 μm in length and 50–70 nm in diameter) bound and impregnated with carbonated apatite nanocrystals (tens of nm in length and width, 2–3 nm in thickness) (14). These fibers are further organized at microstructural length-scales into a lamellar structure with adjacent lamellae being 3–7 μm thick (16). Threaded throughout this lamellar structure are the secondary osteons (31) (up to 200–300 μm diameter), large vascular channels (up to 50–90 μm diameter) oriented roughly along the longitudinal direction of the bone and surrounded by circumferential lamellar rings, with so-called "cement lines" at the outer boundary.

Critical for developing a realistic framework for fracture risk assessment is an understanding of the importance of bone's microstructural hierarchies on its mechanical properties. Indeed, the difficulty in understanding the mechanisms of fracture in bone clearly lies in determining the role that the underlying microstructural constituents and morphology play in crack initiation, subsequent crack propagation and final unstable fracture, and in separating their effects on the critical fracture events. It is the intent of this chapter to describe how fracture mechanics, along with various characterization techniques, have been used to begin developing such a mechanistic framework for the fracture behavior of cortical bone, and, where possible, to relate the specific toughening mechanisms to the underlying nature of the microstructure. The initial focus will be directed to the large body of early literature that addressed these issues by measuring "single-value" fracture toughness behavior, using such parameters as the work of fracture, W_f, the critical stress-intensity factor, K_c, or the critical strain-energy release rate, G_c. Secondly, more recent results that address the fact that cracking in bone involves rising fracture resistance with crack extension will be discussed, in light of the salient mechanisms involved. Finally, the topic of time-dependent damage and fracture is described in terms of the specific mechanisms involved.

2. SINGLE-VALUE TOUGHNESS MEASUREMENTS

2.1. Fracture Mechanics

One method that is used to characterize the toughness of materials uses the work of fracture, W_f, which is obtained by dividing the area under the load-displacement curve measured during the toughness test by twice the nominal crack-surface area. This approach has been used for cortical bone to quantify the toughness of nominally "flaw-free" specimens (8,11,17,25,26,32) but suffers because results can be both specimen size- and geometry-dependent. Consequently, work of fracture results generally are not useful for comparing values determined in different studies that used different sample geometries, but may be used successfully to assess trends when the nominal sample size and geometry are held constant.

Akin to other structural materials, the fracture of bone is better characterized by linear-elastic fracture mechanics. In this case, for an essentially linear-elastic material, where any inelastic (e.g., yielding) behavior is limited to a small near-tip region, the stress and displacement fields local to the tip of a preexisting crack are described by the stress-intensity factor, K. The stress-intensity factor may be defined for mode I (tensile-opening loading), mode II (shear loading), or mode III (tearing or antishear loading) in terms of the geometrical crack configuration, applied stress, σ_{app}, and crack size, a, *viz*. (33):

$$K_{(I,II,III)} = Q\sigma_{app}(\pi a)^{1/2}, \tag{1}$$

where Q is a dimensionless parameter dependent on sample geometry and loading mode (i.e., mode I, II, or III) (Fig. 1). The resistance to fracture, or fracture toughness, is then defined for particular mode of loading as the critical value of the stress intensity, K_c, at the onset of unstable fracture, typically computed from the peak stress. An alternative fracture mechanics description, which has also been used in studies on the toughness of bone, expresses toughness in terms of a critical value of the strain-energy release rate, G_c, defined as the change in potential energy per unit increase in crack area at fracture, which may be expressed as (33):

$$G_c = \frac{P^2}{2B}\frac{dC}{da}, \tag{2}$$

where P is the load, B the specimen thickness, and dC/da is the change in sample compliance with crack extension (the compliance, C, is the slope of the displacement-load curve). It is important to note that for linear-elastic materials, G and K are uniquely related, viz.:

$$G = \frac{K_I^2}{E'} + \frac{K_{II}^2}{E'} + \frac{K_{III}^2}{2\mu}, \tag{3}$$

where E' is the appropriate elastic modulus ($E' = E$ in plane stress, $E/(1-\nu^2)$ in plane strain, where E is Young's modulus and ν is Poisson's ratio), and μ is the shear modulus (33). If linear-elastic conditions prevail (i.e., inelastic deformation is limited to a small zone near the crack tip), both G_c and K_c should give a geometry-independent measure of toughness, provided plane-strain conditions are met, as described below. Some typical mode I fracture toughness values measured for bone, tabulated from various sources, are summarized in Table 1 (13,17,19,26,29,30,32,34–40).

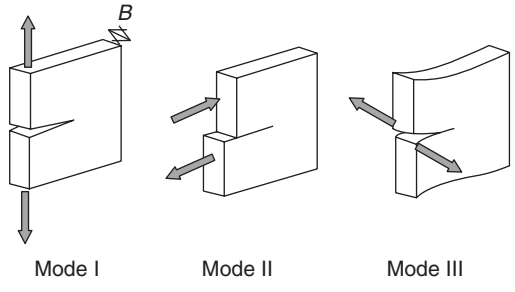

Figure 1. Schematic illustrating the different modes of loading: mode I (tensile-opening loading), mode II (shear loading), and mode III (tearing or antishear loading). Loading *in vivo* could involve one or more of these modes.

2.2. Plane Stress Versus Plane Strain

In applying fracture mechanics, the specimen thickness, B, may affect the measured toughness values as loading conditions change from a state of plane strain to that of plane stress. Plane strain here refers to a condition where the out-of-plane strain is essentially zero, whereas with plane stress, the out-of-plane stress is zero. If the sample has a thickness significantly larger than the scale of local inelasticity, K_c or G_c values should be thickness-, geometry-, and crack-size independent and a condition of plane strain is said to exist. However, with thinner specimens, the toughness values may be significantly higher and not independent of such factors as conditions approach those of plane stress. The ASTM standard for mode I fracture toughness testing of metals (i.e., ASTM E-399) requires that (41):

$$B \geq 2.5\left(\frac{K_I}{\sigma_Y}\right)^2 \tag{4}$$

for plane-strain conditions to exist, where σ_Y is the yield stress of the material. As a result of variations in K_I and σ_Y with factors such as species, location, and orientation, the condition in Equation 4 may not always be strictly met for fracture testing of cortical bone, particularly for human bone, which is of the most clinical interest. For example, based on properties compiled in Ref. 42, thicknesses ranging from ~1–10 mm may be required to meet plane-strain conditions in human cortical bone, depending on location, age, and orientation, demonstrating how Equation 4 may not always be easily satisfied for all practical testing. It should be noted, however, that Equation 4 is typically considered conservative for most engineering materials and its specific relevance to cortical bone has not been thoroughly explored. In an early study, no thickness dependence was found for mode I longitudinal cracking (see Fig. 2 for details on orientation designation) in bovine femora for 1.8–3.8-mm thick specimens (36); a similar conclusion was reached for mode I fracture of bovine tibia, also in the longitudinal direction, where no thickness dependence was seen between 0.5 and 2 mm (37). Conversely, more recent studies by Norman et al. report that the mode I toughness varied significantly with thickness from 2–6 mm, becoming essentially constant after a thickness of 6 mm was achieved (38). Limited experiments on human tibia also showed little change in mode I toughness for 2–3-mm thick specimens (38). Thus, until more extensive information on this subject is available, caution should be used when comparing fracture data on bone from different studies that used appreciably different specimen thicknesses.

Table 1. Examples of Mode I Single-Value Fracture Toughness Results for Cortical Bone Taken from Various Sources

Species	Bone	Orientation[§]	K_c (MPa$\sqrt{m}$)	G_c (J/m^2)	Test Geometry	Ref.
Bovine	Femur	Long	3.6 ± 0.7		C(T)	36
Bovine	Femur	Long	2.4–5.2[*]	920–2780	C(T)	34
Bovine	Femur	Transverse	5.7 ± 1.4		SEN(B)	40
Bovine	Femur	L-R	3.4–5.1[#]		SEN(B)	32
Bovine	Femur	C-L	2.1–2.9[#]		SEN(B)	32
Bovine	Tibia	Long	4.5–5.4[*]	760–2130	C(T)	35
Bovine	Tibia	Long	2.8–6.3[*]	630–2880	C(T)	37
Bovine	Tibia	Long	3.2		C(T)	39
Bovine	Tibia	Transverse	6.4		C(T)	39
Bovine	Tibia	L-R	4.5–6.6[#]		SEN(B)	32
Baboon	Femur	Long	1.8 ± 0.5		C(T)	30
Baboon	Femur	Transverse	6.2 ± 0.7		SEN(B)	30
Baboon	Femur	Long	1.7–2.3[*Dagger*]		C(T)	13
Human	Femur	L-C	6.4 ± 0.3		SEN(B)	17
Human	Femur	C-L		520 ± 190	C(T)	19
Human	Tibia	C-L		400 ± 250	C(T)	19
Human	Tibia	C-L	4.1–4.3[†]	600–830	C(T)	38
Human	Humerus	C-R	2.2 ± 0.2		SEN(B)	29
Human	Humerus	C-L	3.5 ± 0.1		SEN(B)	29
Human	Humerus	L-C	5.3 ± 0.4		SEN(B)	29
Human	Femur	Transverse	4.3–5.4		SEN(B)	26

Data are given in either K or G as reported by the authors. All reported values are mean values, standard deviations are given when possible.
[§]When specific orientation is unknown, cracking direction is given, see Fig. 2 for details.
[*]Range of mean values for several sets of data from samples tested at different loading rates.
[†]Range of mean values for two sets of data using samples of different thickness.
[‡]Range of mean values for three sets of data using samples from different age groups.
[#]Range of mean values for two sets of data using samples stored in different media.

2.3. Effect of Loading Mode

Similar to most engineering materials, cortical bone shows the least resistance to fracture under mode I loading. Indeed, Norman et al. has shown average ratios of G_{IIc}/G_{Ic} to be 12.7 and 4.6 for longitudinal (C-L) fracture in human tibia (43) and femur (10), respectively, for donors aged between 50 and 90 years. Similarly, higher G_{IIc} values relative to G_{Ic} have been reported for human femoral neck as well (22). A recent study focused on mode I, II, and III fracture in bovine femora found G_{IIc}/G_{Ic} and G_{IIIc}/G_{Ic} to be 3.8 and 2.6, respectively, for longitudinal fracture and 3.4 and 2.9, respectively, for transverse fracture (44). Although such results suggest mode III fracture may be easier than mode II, it is unclear whether this will be true for all species, locations, orientations, and other variables. As mode I fracture is the easiest failure mode, it has received the most attention in the literature and, accordingly, will be the subject of the rest of this chapter.

2.4. Effect of Orientation

Studies concerning the effect of orientation on the toughness of bone (Fig. 2) have shown transverse cracking directions (L-C and L-R) (i.e., where the crack must cut the osteons) to be consistently tougher than orientations with longitudinal cracking (C-L and R-L), where the crack splits osteons along the longitudinal axis of the bone. In bovine tibia, Behiri and Bonfield demonstrated a progressive increase in toughness (from 3.2 to 6.5 MPa$\sqrt{m}$) as the orientation of specimens was varied rotationally from the longitudinal to transverse cracking directions (39). This effect was quite strong, such that side grooving of specimens was required to achieve straight crack propagation in all but the longitudinal case, otherwise cracks would kink toward the longitudinal direction (e.g., Fig. 3). Indeed, K_{Ic} for transverse cracking was found to be up to twice that for longitudinal cracking in bovine tibia (32,39) and femora (32,44). Furthermore, a study on baboon femora showed an even larger effect, with a mean K_{Ic} for fracture in the transverse direction some 3.5 times higher than in the longitudinal direction (30). Finally, in human humeri, similar behavior has been observed, with cracks kinking $\sim 90^\circ$ toward the longitudinal direction (anatomically proximal-distal) when cracking in the transverse direction was attempted, with transverse toughness (L-C) reported to be 1.5 times the longitudinal (C-L) (5.3 versus 3.5 MPa$\sqrt{m}$); conversely, the C-R orientation, which splits the osteons along the short axis, showed the lowest toughness of 2.2 MPa$\sqrt{m}$ (Fig. 4) (29). It should be noted that the latter two studies did not use specimen side grooving to ensure cracking in the transverse directions (Fig. 3), and accordingly the transverse toughness values may be lower bounds (i.e., the orientation effect may be even larger than was reported in those studies). Fracture toughness results for different orientations may be found in Table 1.

2.5. Effect of Anatomical Location

Although comparisons of data from many different studies may suggest differences in toughness with bone location, it is difficult to separate other variables that might be involved to determine the significance of such differences. One study compared the toughness of femoral neck, fem-

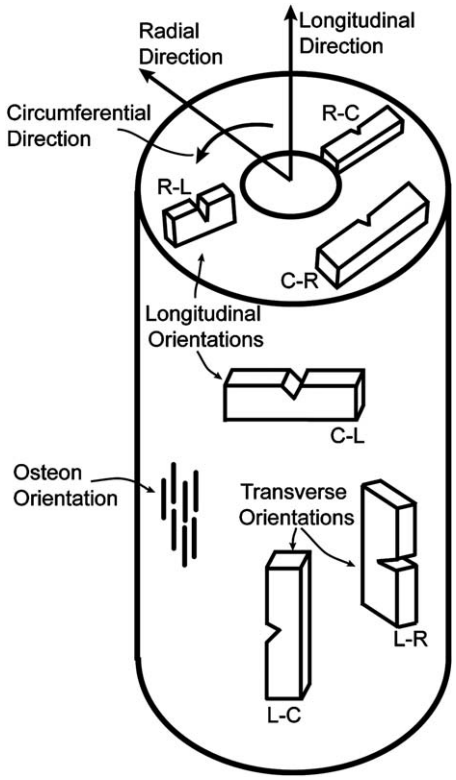

Figure 2. Schematic illustrating the orientation code used by the ASTM E399 fracture toughness standard (41). The first letter in the designation refers to the normal direction to the crack plane, whereas the second letter refers to the expected direction of crack propagation. It is seen that the L-C and L-R orientations involve transversely cutting the osteons, and accordingly, these orientations are commonly referred to as having a transverse cracking direction in the literature. Conversely, orientations that split apart the osteons along the longitudinal axis (R-L and C-L) are commonly referred to as orientations with longitudinal cracking. Often, the specific transverse or longitudinal orientation is not given; however, the L-C and C-L orientations are the easiest to machine, especially from smaller bones. Finally, the orientations splitting the osteons along their short axes (C-R and R-C) are the least common orientations found in the fracture literature.

oral shaft, and tibial shaft specimens from matched human cadeveric bones in order to isolate the effect of bone location (19). For identically sized C-L oriented specimens, the femoral shaft demonstrated significantly higher average G_{Ic} values relative to tibial shaft specimens (520 versus 400 J/m^2). Although difficulties existed in comparing femoral neck data directly because of sample size restrictions, results suggested a significantly higher toughness than both the femoral and tibial shaft specimens. Thus, it appears that bone location does indeed have an effect on toughness; however, it is not yet clear what microstructural differences associated with various locations may cause such toughness changes. Some toughness results for different anatomical locations within the same species can be found in Table 1.

Figure 3. Optical micrograph illustrating $\sim 90^\circ$ crack deflection for an L-C oriented specimen into the longitudinal direction (indicated by white arrows) along a cement line in human cortical bone taken from the humerus.

2.6. Effect of Age

A critical issue with bone fracture is the problem of aging. Indeed, a large number of studies that have looked at age-related issues in the mechanical properties of bone have implied a significant deterioration of the fracture tough-

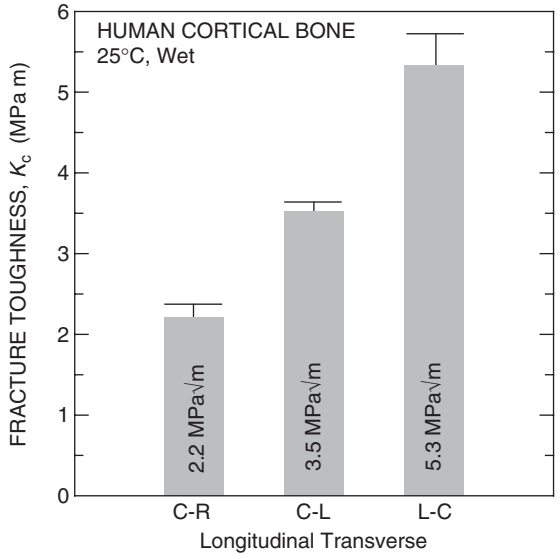

Figure 4. Variation in fracture toughness with orientation in human humeral cortical bone. Note the significantly higher toughness for the transverse (circumferential) orientation. The toughness in the transverse (L-C) case was ascribed to deflection of the crack because of the strong role of the cement line in that orientation (29).

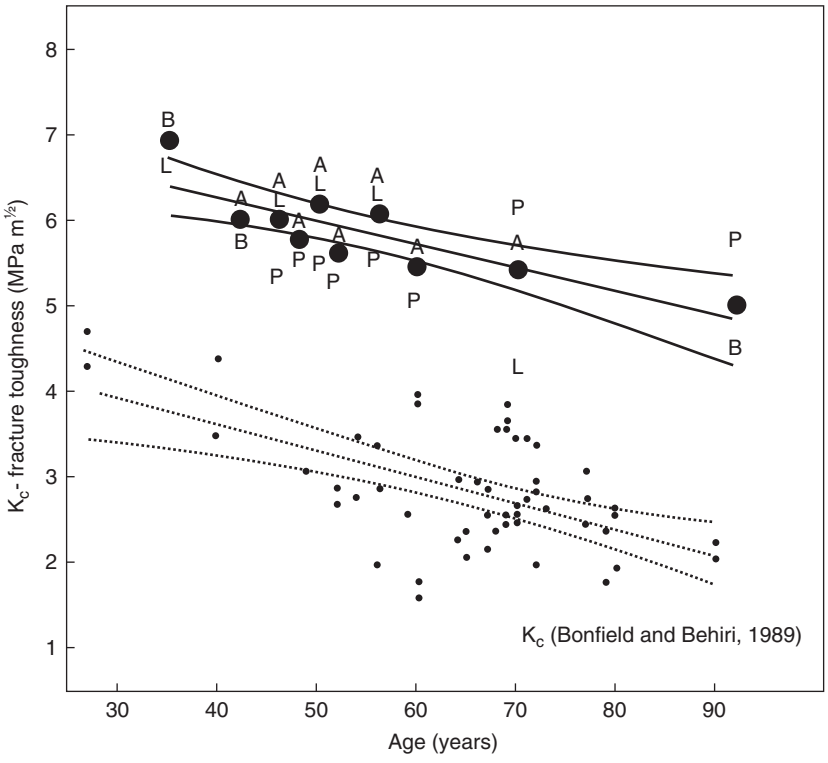

Figure 5. Variation in fracture toughness with age in human cortical bone. Data for transverse (circumferential) (L-C) crack growth in femoral bone (top) and for longitudinal (C-L) crack growth in tibial bone (bottom) are included. Note the clear trend of decreasing toughness with age and the effect of orientation is consistent with that previously discussed [courtesy: Zioupos and Currey (17)].

ness with age (8–11,13,17,19,22,26,30,45–47). Some results showing this trend may be seen in Fig. 5 (17). In particular, aging has been associated with increased mineralization (46) and lowered collagen network integrity (26), with resultant reduction in the elastic deformability and toughness (5,13,17,19,26,30,46). Also, it has been suggested that remodeling induced by increasing microdamage with aging (4) leads to an increase in the difference in properties of the matrix (primary lamellar bone) and the secondary osteons, implying a stronger role for the cement lines and a reduction in the toughness (5,17,23,30). Thus, a desire exists to understand the fracture properties of bone as a function of age. Indeed, if specific age-related changes within the microstructure of bone can be linked to a reduced fracture resistance, progress can be made toward creating successful treatments to combat these deleterious effects, which has led to numerous studies centered on the role of microstructural changes in affecting the fracture toughness, as discussed below.

2.7. Effects of Microstructural Factors

It has long been observed that changes in bone density and mineral content may be associated with changes in the toughness of bone; indeed, studies on human and bovine bone have reported increases in toughness with increasing dry and wet density (15,22,36), and decreases in toughness with increasing mineral content (8,11) or porosity (12). Although such results support the notion that bone fragility and osteoporosis may be associated with such factors, more recently it has become increasingly apparent that these factors alone cannot explain, for example, gender differences in fracture rates (48) and why antiresorptive drugs can lower fracture risk independent of bone mineral density (6,7). Furthermore, there have also been studies that show fracture toughness to be independent of bone density or mineral content (13,30,49), even when decreases in toughness with age were observed (13,30).

In light of this information, excessive remodeling has been suggested as a possible cause for increasing fracture risk with age (6,7); such remodeling can lead to loss in bone mass, but more importantly may also result in other morphological changes to the microstructure of bone. With regard to these microstructural factors, fractographic studies have suggested that *in vivo* and *in vitro* fracture occurs more readily in human bone where fewer and smaller osteons exist (50). An *in vitro* fracture toughness study of longitudinal cracking in human femur and tibia specimens found higher toughness with smaller osteons and increasing osteonal density (12); however, no significant relationships with these factors could be found for femoral neck specimens (22), which did not show a decrease in toughness with age.

The cement line, the boundary between secondary osteons and the surrounding lamellar matrix, is another microstructural element thought to play a key role in the fracture of bone. Indeed, both microcracks and macroscopic cracks have been observed to deflect along the cement lines upon encountering osteons (Fig. 3), leading to the conclusion that the cement line must provide a weak path for fracture (23,29,51–54). Furthermore, the weak path provided by the cement lines may be responsible for the strong orientation effects seen in the fracture of bone (see section on Effect of Orientation) (i.e., the crack deflection of transverse cracks toward the longitudinal di-

rection is likely because of the cement lines), as suggested in Refs. 29,30.

Finally, changes in the mechanical properties of the microstructural constituents, such as collagen, may also have a significant effect on fracture resistance. Research into the effect on the fracture toughness of collagen denaturation, achieved both thermally and chemically (25,55), found significant decreases in the work of fracture of human femur specimens with increasing amounts of denaturation. Another study on the effect of storage in alcohol vs. saline (32) reported an elevation in toughness with storage in alcohol. It has been suggested that storage in a similar solvent (methanol) increases the collagen cross-link density in demineralized dentin (56); it is conceivable that a similar phenomenon is responsible for the observations in Ref. 32.

3. RESISTANCE-CURVE BEHAVIOR

Although the use of a single-value measure of the toughness, as has been discussed so far, is appropriate for many materials, in cases where specific extrinsic toughening mechanisms are active, such as in bone, the fracture resistance actually increases with crack extension, thereby promoting stable crack growth and requiring a so-called resistance-curve (R-curve) fracture-mechanics approach (33,57). This approach can be understood by appreciating that crack propagation is governed by two distinct classes of mechanisms: *intrinsic* mechanisms, which are microstructural damage mechanisms that operate ahead of the crack tip, and *extrinsic* mechanisms, which act to "shield" the crack from the applied driving force and operate principally away from the crack tip, in a frontal process zone or in the crack wake (58–60). R-curve behavior is the natural result of extrinsic toughening, as the toughness is a function of the length of the crack wake (58–60). Examples of such extrinsic mechanisms seen in engineering materials are crack bridging, phase transformations, and constrained microcracking, all of which develop as the crack extends (Fig. 6). In such instances, crack extension commences at a *crack-initiation toughness,* K_o, while sustaining further crack extension requires higher driving forces until a "plateau" or steady-state toughness is often reached. The corresponding slope of the R-curve can be considered as a measure of the *crack-growth toughness*. Although important for understanding the fracture behavior of bone, R-curve analysis is also important for understanding the intrinsic and extrinsic mechanisms involved in fracture, which is discussed in the current and following sections.

Several recent studies (21,28,53,61–65) have revealed rising R-curve behavior in bone (Fig. 7) (53,61,62,64,65), indicative of the presence of active extrinsic toughening mechanisms in the crack wake. One of the first R-curve studies in bone, by Vashishth et al. (64) (Fig. 7a), looked at crack propagation in human and bovine tibia (human donor: 59 years old) for cracking in the longitudinal (proximal-distal) direction. It was found that the toughness of human and bovine bone specimens rose linearly from 1.6 to 2.5 $\text{MPa}\sqrt{\text{m}}$ and from 3.9 to 7.2 $\text{MPa}\sqrt{\text{m}}$, respectively, over crack extensions of $\sim$2.25 mm. Thus, K_o was found to be 1.6 and 3.9 $\text{MPa}\sqrt{\text{m}}$ for human and bovine bone, respectively. A more recent study by Pezzoti and Sakakura

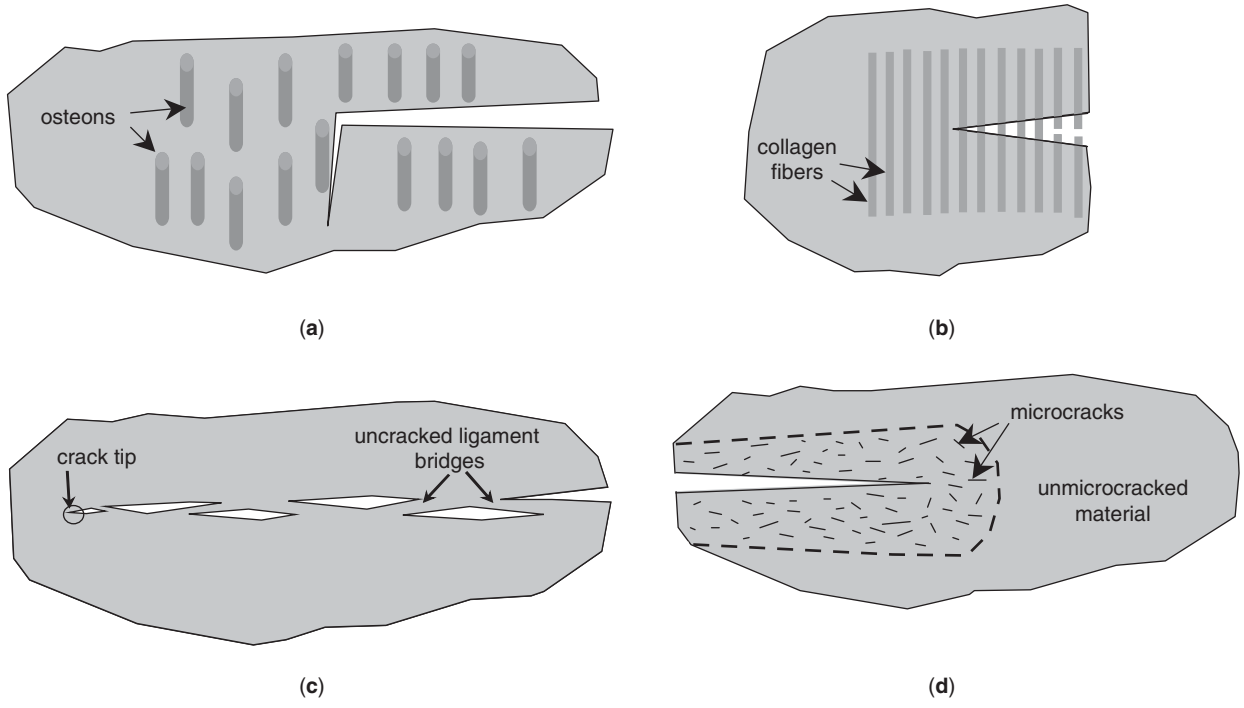

Figure 6. Schematic illustrations of some of the toughening mechanisms possible in cortical bone: (a) crack deflection (by osteons), (b) crack bridging (by collagen fibers), (c) uncracked ligament bridging, and (d) microcracking. One or more of these mechanisms can be expected to be active.

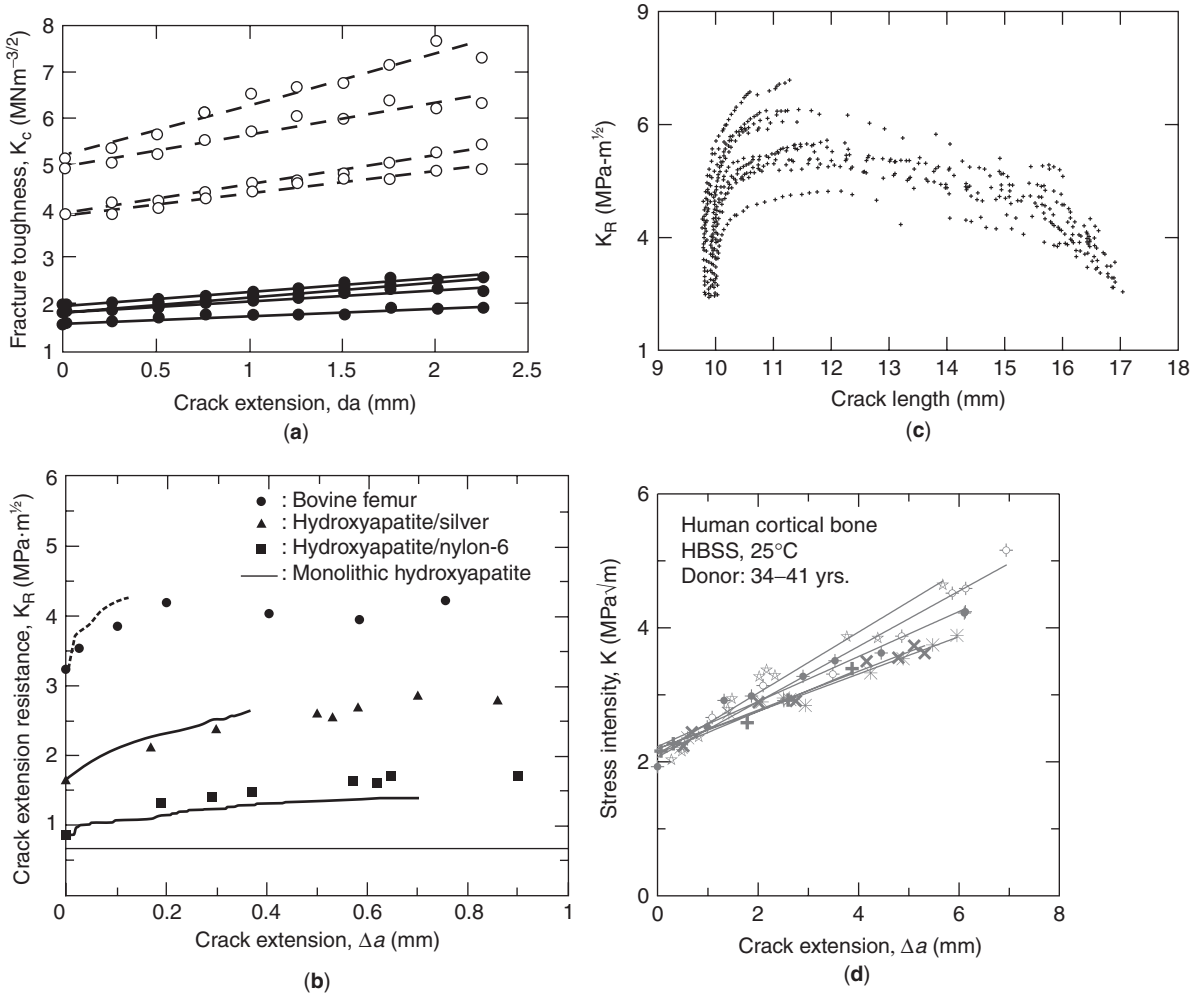

Figure 7. Resistance curve data for: (a) human (solid points) and bovine (hollow points) [courtesy: Vashishth et al. (64)], (b) bovine bone [courtesy: Pezzotti and Sakakura (61)], (c) equine bone [courtesy: Malik et al. (65)], and (d) human bone [courtesy: Nalla et al. (53,62)]. Note the initial rising R-curve behavior in each case (supporting existence of active extrinsic toughening mechanisms), although subsequent behavior may differ.

(61) also reported a rising R-curve in bovine bone; however, after an initial rising portion, a steady-state (so-called "plateau" toughness) was achieved, typical of many materials that exhibit R-curve behavior (Fig. 7b). These authors reported values of ~ 3.2 MPa$\sqrt{\text{m}}$ and ~ 5 MPa$\sqrt{\text{m}}$/mm for the initiation toughness and the (initial) slope, respectively. Similarly Malik et al. (65) reported rising R-curve behavior for transverse crack growth in equine bone (Fig. 7c); here, R-curves reached a steady-state plateau, and in some cases decreased, with mean K_o values of ~ 4.38–4.72 MPa$\sqrt{\text{m}}$ and mean slopes (calculated from mean parameters reported in Ref. 65) of 1.06–2.57 MPa$\sqrt{\text{m}}$/mm. Additionally, linearly rising R-curve behavior, with no apparent plateau, has been reported for cortical bone from red deer antler (28).

The most recent work on R-curve behavior in human bone involved longitudinal (proximal-distal) crack growth, using the C-L orientation, in humeral bone (Fig. 7d: donors 34–41 years old); an average crack-initiation toughness, K_o, of 2.06 (S.D. = 0.19) MPa$\sqrt{\text{m}}$ with the R-curves monotonically rising over 5–7 mm (no plateau), with a mean slope of 0.39 (S.D. = 0.09) MPa$\sqrt{\text{m}}$/mm, was reported (53,62). These toughness results are slightly higher than those of Vashishth et al. (64) for 59-year old human tibial cortical bone tested in the same proximal-distal orientation, where K_o values of ~ 1.6–1.9 MPa$\sqrt{\text{m}}$ and slopes of ~ 0.13–0.27 MPa$\sqrt{\text{m}}$/mm were measured. These differences may be the result of age-related variations in the bone tissue, which were discussed earlier and will be addressed in further detail for R-curves below.

Recently, results demonstrating the effects of aging on R-curve behavior in human bone (C-L orientation) have been reported (66). Results for three distinct age groups (34–41 years, 61–69 years, and 85–99 years) are presented in Fig. 8 (66) and clearly indicate a degradation in the toughness of bone with age. Specifically, the crack-initia-

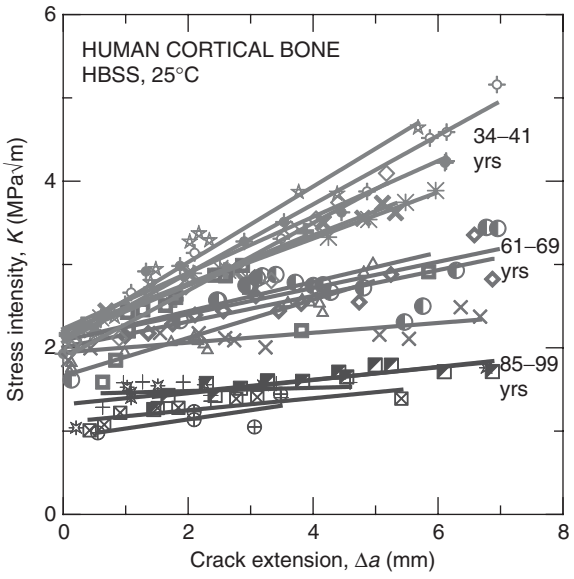

Figure 8. Effect of aging on the resistance curve behavior of human cortical bone. A decrease in the initiation toughness with age exists and the growth toughness (reflected by the slope of the R-curves) is essentially eliminated over the range of ages investigated [courtesy: Nalla et al. (66)].

tion toughness, K_o, decreased from 2.06 (S.D. = 0.19) MPa$\sqrt{}$m for the 34–41 year group to 1.96 (S.D. = 0.18) MPa$\sqrt{}$m for the 61–69 year group to 1.22 (S.D. = 0.20) MPa$\sqrt{}$m for the 85–99 year group. The slope of the R-curve, which reflects the crack-growth toughness, also decreased from 0.39 (S.D. = 0.09) MPa$\sqrt{}$m/mm for the 34–41 year group to 0.16 (S.D. = 0.06) MPa$\sqrt{}$m/mm for the 61–69 year group to 0.07 (S.D. = 0.03) MPa$\sqrt{}$m/mm for the 85–99 year group. For comparison, the toughness data of Vashishth et al. (64) for 59-year old human tibial cortical bone, tested in the same proximal-distal orientation, agrees very well with these trends with K_o values of $\sim$1.6–1.9 MPa$\sqrt{}$m and slopes of $\sim$0.13–0.27 MPa$\sqrt{}$m/mm being reported, although it is possible that anatomical location (tibia vs. humerus) may be a confounding variable. These results clearly indicate that a decrease in the initiation toughness with age not only exists, but a decrease in the crack growth toughness exists as well. It should be noted that it is the combination of these two factors that contribute to the reported declines in single-value (overload) toughness with age discussed earlier. Nevertheless, it is important to understand these changes on a micromechanistic level, and specifically how any variation in microstructure associated with aging may separately affect the intrinsic and extrinsic toughening mechanisms. Some progress has been made in this regard, as discussed in the next section.

4. MECHANISTIC ASPECTS OF FRACTURE

4.1. Intrinsic Mechanisms of Fracture

Historically, models for bone fracture have been based on the concept of the critical fracture event being strain-controlled (67–69) (i.e., that fracture occurs when some critical strain (as opposed to a critical stress) is locally achieved). Recently, experiments have been conducted to verify this hypothesis. Using a double-notched four-point bend geometry, Nalla et al. showed that the onset of the *local* fracture events in cortical bone is consistent with strain-controlled fracture by noting that crack initiation occurred at points of maximum strain, as opposed to points of maximum stress (29).

The intrinsic fracture mechanisms for cortical bone are poorly understood; however, several important factors that are thought to affect the intrinsic toughness may be identified. First, the cement lines within the bone microstructure are thought to provide an intrinsically weaker path for fracture relative to the rest of the microstructure, as mentioned earlier and evidenced in Fig. 3. Accordingly, the local properties of the cement lines should play a prominent role in determining the overall intrinsic toughness of cortical bone for many loading configurations. Indeed, the higher density of osteons, and their associated cement lines, in older bone may be a significant factor in causing the degradation in intrinsic toughness with aging (66,70). Additionally, another factor that likely leads to the aging-related decrease in the intrinsic toughness is a degradation in the quality of the collagen, a factor that has also been implicated in deterioration of mechanical properties of demineralized bone (71). Indeed, nanoindentation and atomic force microscopy results indicate that the structure and mechanical properties of collagen from older bone (85–99 years old) are significantly deteriorated when compared with younger bone (34–41 years old) (70). Furthermore, deep ultraviolet Raman spectroscopy results suggest changes in the collagen molecular bonding consistent with an increase in the nonreducable cross-link content with aging, providing further evidence that changes in the collagen may be related to the lower observed toughness (70).

4.2. Extrinsic Toughening Mechanisms

In contrast to the intrinsic mechanisms of fracture, far more progress has been made in understanding the mechanisms of extrinsic toughening in bone, which are responsible for the rising R-curve behavior (see section 3). Extrinsic toughening mechanisms act away from the crack tip, in the surrounding material or in the crack wake, and cause a local reduction in the stresses felt at the crack tip. Although early studies attributed the rising toughness with crack extension observed in bone to the mechanism of constrained microcracking (21,28,64), more recently it has been shown that crack bridging is in fact the primary mechanism responsible for such behavior (29,53,61,62), where intact bridges of material across the crack sustain part of the applied load (Fig. 9) (29). As at first glance these mechanisms may sound similar, it is important to understand the differences in the mechanics

involved with each mechanism. With constrained microcracking, the formation of microcracks is in the damage zone ahead of the crack tip; this damage zone is left in the wake of the crack as it extends, and is reasoned to increase the (extrinsic) toughness because of (1) the volume expansion within the damage zone from the formation of microcracks, which if constrained by surrounding rigid material exerts a compressive stress at the crack tip, and (2) the reduction in modulus that occurs within this zone (72,73). However, these effects are offset at least in part by the presence of a microcracked region ahead of the crack that can act to lower the intrinsic toughness. Indeed, a lower toughness has been observed in highly microcracked bone (74), indicating that the benefits of extrinsic toughening would need to be high for this mechanism to be effective. As a general toughening mechanism, the toughening effects of microcracking are invariably small, and the mechanism has largely been discounted as a significant source of toughening in all but a few multiphase ceramic materials with high internal residual stresses (75).

In contrast, crack bridging is a toughening mechanism where uncracked material bridges the crack wake and sustains part of the applied load that would otherwise contribute to crack growth. In bone, this bridging occurs in the form of so-called uncracked ligaments, often hundreds of micrometers in size, or by individual collagen fibrils over much smaller dimensions (29,53,61,62,76). Uncracked ligament bridges have been shown to provide the majority of extrinsic toughening that contributes to R-curve behavior (53,62), whereas collagen fiber bridging is hypothesized to play a role in resisting the propagation of microcracks (76). The uncracked ligaments provide a particularly potent form of toughening and are created either by the nonuniform advance of the crack front or by the imperfect linking of microcracks, which initiated ahead of the crack tip, with the main crack. Thus, although microcrack formation may lead to bridging, the mechanics of the two mechanisms are quite different. Crack bridging acts to reduce the stress intensity experienced at the crack tip, K_{tip}, relative to the applied stress intensity, K_{app}, by an amount typically referred to as the bridging stress intensity, K_{br}, viz:

$$K_{tip} = K_{app} - K_{br}. \tag{5}$$

The reduction in stress intensity is because bridges in the crack wake sustain a portion of the applied load. As bridges develop with crack extension, K_{br} increases with crack extension as well, resulting in rising R-curve behavior. A steady-state "plateau" toughness may be reached under conditions where bridges are created and destroyed at the same rate, at which point K_{br} essentially becomes constant.

For human and bovine bone, examinations using both microscopy (Fig. 9) and x-ray tomographic techniques (Figs. 10 and 11) (29,53,61,62,66) has verified the existence of both collagen fiber bridges near the crack tip and uncracked ligament bridges far into the crack wake. Furthermore, characterization of such bridging in bone have revealed that, in human humeri, bridging zones containing uncracked ligament bridges extend some 5–6 mm behind the crack tip, and that such bridges do indeed sustain load (53). Specifically, quantitative estimates of the contribution of bridging to the toughness of human humeri have been made using both experimental compliance data and theoretical bridging models (53,62). Such results were in agreement with actual levels of toughening observed from R-curve measurements, with $K_{br} \sim 1$–$2.5\,\mathrm{MPa}\sqrt{\mathrm{m}}$.

Experiments have also been conducted to assess the bridging stresses in the crack wake in bone. Pezzotti et al.

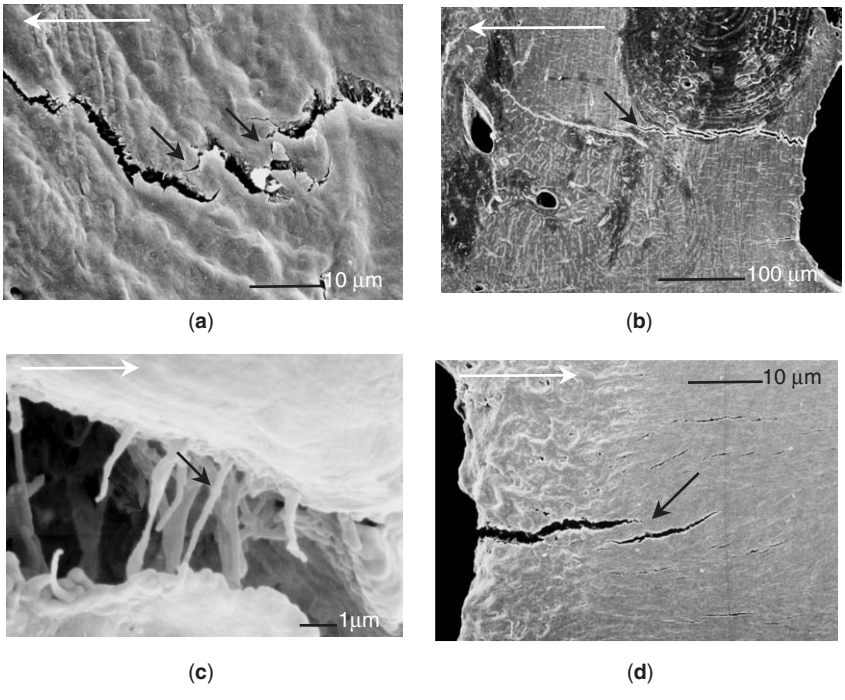

Figure 9. Scanning electron micrographs illustrating crack bridging. For the transverse (radial) orientation, (a, b) evidence of uncracked ligament bridging (indicated by black arrows), and (c) possible collagen fibril-based bridging (indicated by black arrows). For the longitudinal orientation, (d) evidence of uncracked ligament bridging (indicated by black arrow). The white arrows in (a)–(d) indicate the direction of nominal crack growth [courtesy: Nalla et al. (29)].

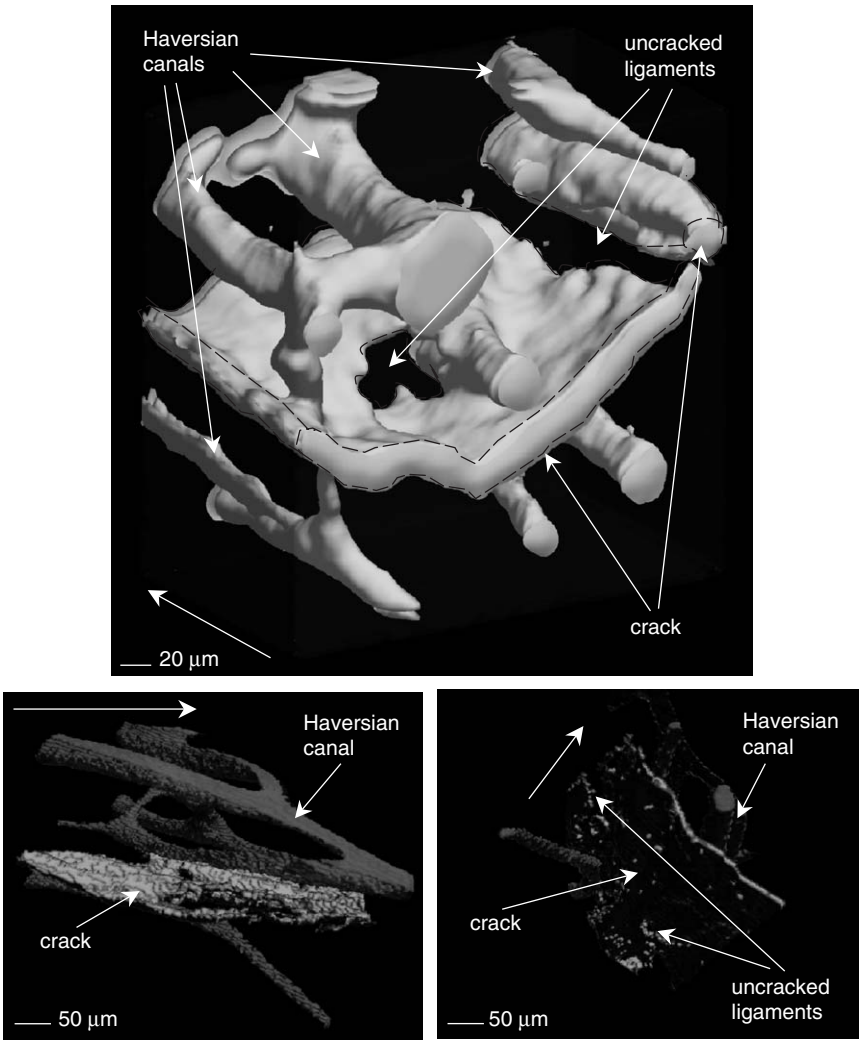

Figure 10. 3D tomographic reconstructions of sections of a crack in the longitudinal orientation are shown. Note that the crack appears to follow the cement lines bordering the osteons. Uncracked ligaments are indicated. The white arrow in each case is the direction of nominal crack growth [courtesy: Nalla et al. (50)].

(61) used Raman microprobe spectroscopy to measure bridging stresses over a distance of 100 μm behind a crack tip in bovine femur. Results indicated stresses as high as 200–300 MPa within the first 10 μm of the crack tip, but falling off to ∼10–50 MPa at a distance of 100 μm behind the tip. Such results gave highly localized measurements, with a 1 μm probe diameter, measuring to a depth of 20 μm. Using compliance-based experiments, estimates of the average through-thickness bridging stresses were also made for human humeri (53). From this study, average peak bridging stresses were found to be in the range 7 to 17 MPa near the crack tip, and to decay over distances of 5 to 6 mm within the bridging zones in the crack wake. The lower bridging stresses deduced in the latter study may in part be because of species variation; however, more importantly, it must be considered that the average through-thickness behavior is measured in that case. Accordingly, although the stresses may be very high locally for discreet bridges, when the through-thickness behavior is considered, it is offset by surrounding unbridged regions unable to support any load (see Ref. 53).

With regard to aging effects on crack bridging, R-curve results show a clear decrease in the extrinsic toughening contribution (i.e., K_{br}) for older bone (Fig. 8). Two likely factors exist that govern this loss of extrinsic toughening, namely a reduction in the number of bridges or the quality of the bridges that form in aged bone (66,70). With regard to the former, direct observations of fewer and smaller bridges behind crack tips in aged (85–99 years old) relative to younger (34–41 years old) bone have been made using x-ray tomography (Fig. 11). Indeed, Fig. 11c clearly shows that that fewer bridges exist at given location behind the crack tip and that the bridging zone extends a shorter distance. Additionally, as discussed, evidence mounts that the stiffness of individual collagen fibers is lower in older bone (70), a factor that would decrease the load-bearing capacity of bridges in the crack wake and correspondingly lower the toughening contribution. Furthermore, bridges composed of degraded collagen may be weaker and break prematurely, a factor that may contribute to the lower quantity of bridges seen in older bone. However, it is apparent that much must still be determined, and both quantitative and qualitative assessments of the role of bridging are currently being undertaken in order to achieve an improved mechanistic understanding of the aging effect on bone fracture.

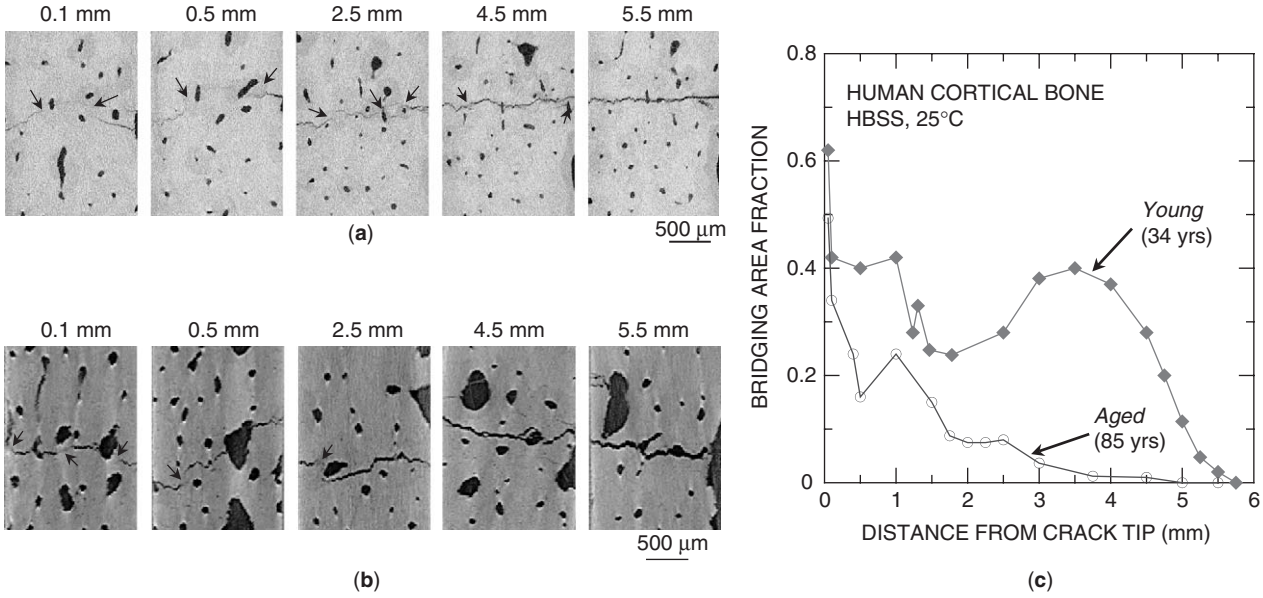

Figure 11. 2D tomographic reconstruction slices showing typical cracks in specimens taken from the (a) *Young* (34FL) and (b) *Aged* (85FR) groups at spaced intervals from the crack tip. Black arrows point out several uncracked ligament crack bridges. (c) The fraction of such bridges with distance from the crack tip quantitatively showing the smaller bridge area fractions and bridging-zone size in the older bone [courtesy: Nalla et al. (66)].

5. TIME-DEPENDENT FRACTURE

Although most clinical fractures are the result of a single overload, or dynamic, fracture event, clinical significance exists for fractures that occur over time (i.e., stress fractures) as a result of periods of sustained loading or cyclic loading (5,77–79); the resulting stable cracking is known as subcritical crack growth. Stress fractures are a well recognized clinical problem with incidence rates of 1–4% often being reported (5,78), with even higher rates cited for adolescent athletes and military recruits (5,77,79). They are commonly seen within a few weeks of a sudden systematic increase in the loading patterns experienced by the bone, when the time elapsed is insufficient for an adaptational response to alleviate the deleterious effects of the increased stress levels (5). In addition, cyclic loading can be a factor in so-called "fragility" fractures commonly seen in the elderly, where increased fracture risk exists because of reduced bone quality as a result of osteoporosis (5).

Early data on subcritical cracking under sustained quasistatic loading came from studies on bovine tibia and femur specimens where the effects of crack velocity on cortical bone toughness in the longitudinal direction were investigated. Results showed higher driving forces (K or G) were needed to grow cracks at higher velocities over the range of $\sim 10^{-5}$–10^{-3} m/sec (34,35,37). Attempts to grow cracks at faster rates resulted in catastrophic failure, along with a change in fracture morphology and a lower toughness. More recent studies (53) that have focused on slow crack growth in human humeri, also in the longitudinal (C-L) direction, report similar results but over a much larger range of growth rates ($\sim 10^{-9}$–10^{-4} m/sec); higher stress intensities were again needed to grow cracks at higher growth rates (Fig. 12) (53). Such behavior is analogous to that displayed by many engineering materials, such as ceramics and metals, which can exhibit time-dependent crack growth under sustained quasistatic loading (33,57). In engineering materials, such behavior is typically associated with environmental effects, although it is unclear what role, if any, the physiological environment plays in subcritical cracking behavior in cortical bone. A peculiar feature observed in cortical bone, however, is that at growth rates below $\sim 10^{-9}$ m/s, significant crack blunting (crack-tip rounding) occurs that eventually leads to crack arrest (Fig. 13) (53). Thus, even without remodeling, bone has a mechanism to arrest the growth of subcritical cracks driven by static (noncyclic) loads.

Cyclic loading also can lead to subcritical crack growth; indeed, fatigue failures have been studied quite extensively in cortical bone, particularly because fatigue damage is considered to be of key importance in understanding stress fractures (2,5,27,42,74,80–104). In traditional terms, fatigue is typically characterized in terms of the

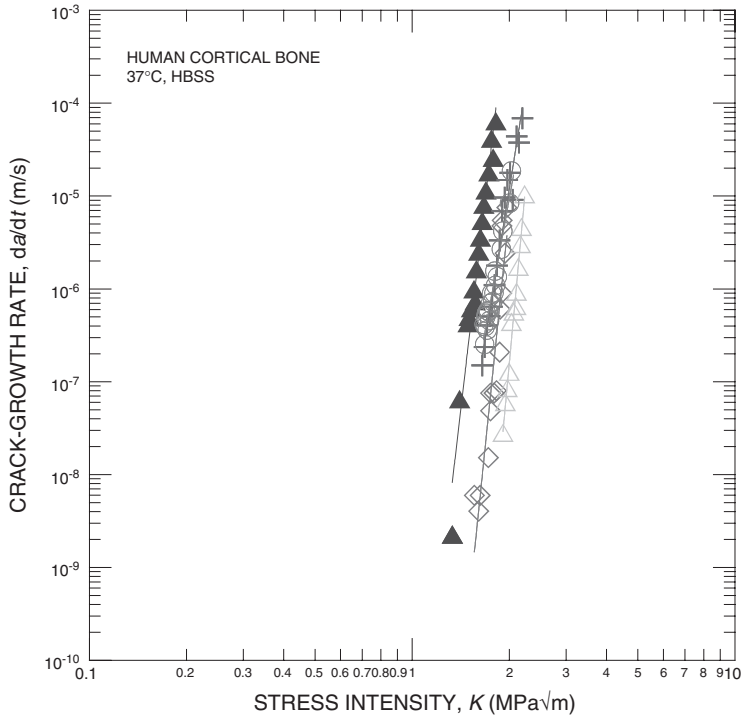

Figure 12. Results showing the time-dependent subcritical crack-growth behavior of human cortical bone, in terms of the growth rates, da/dt, as a function of the stress intensity, K, for growth rates $>10^{-9}$ m/s. Attempts at acquiring data for growth rates $<10^{-9}$ m/s were unsuccessful owing to substantial crack blunting over the time scales involved [courtesy: Nalla et al. (53)].

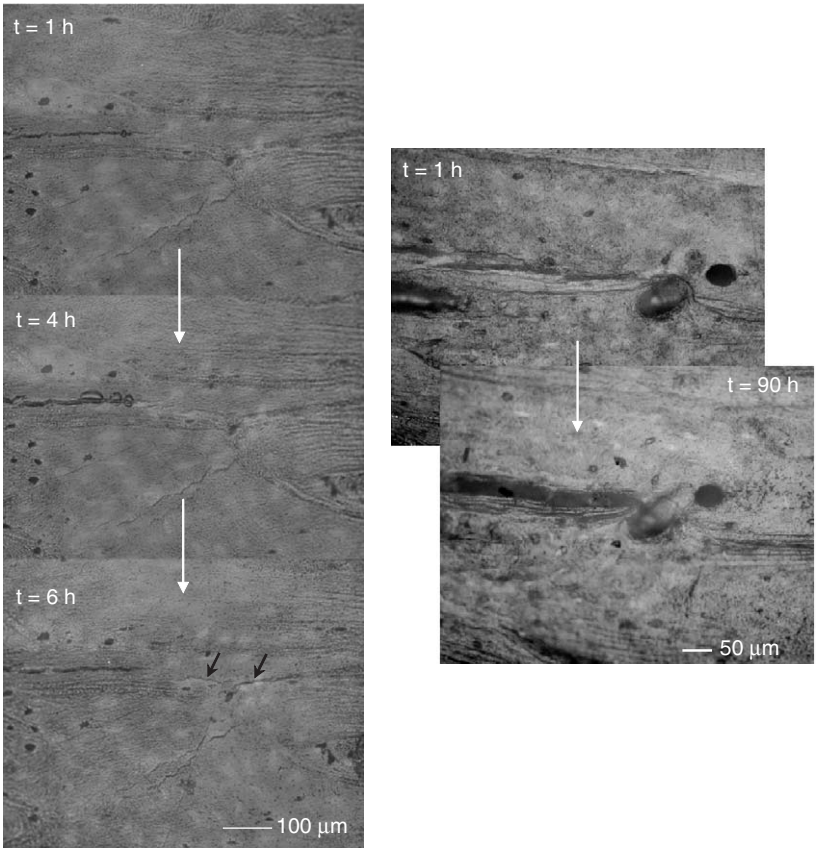

(**a**)

Figure 13. Time-elapsed optical micrographs showing the (a) time-dependent crack extension (clearly seen in bottom micrograph, as indicated by black arrows) that occurs over a time scale of several hours, and (b) time-dependent crack blunting behavior in human cortical bone. Note also the evidence of uncracked ligament bridging and the lack of crack blunting on the shorter time scale in (a). The direction of nominal crack growth is from left to right [courtesy: Nalla et al. (53)].

total life to failure as a function of the alternating stress, termed the *stress-life* or "*S*/*N*" approach. This method involves the estimation of the number of cycles required to induce complete failure of a (nominally flaw-free) "smooth-bar" specimen under prescribed stress levels, where the measured fatigue lifetime represents the number of the cycles both to initiate and propagate a (dominant) crack to failure[1] (105). Such an approach has been widely used for bone to investigate a wide variety of issues, including age (89), donor species (90), cyclic frequency (42,83,96,106), testing geometry (42,89,93), loading mode (88,95,99), fatigue-induced damage accumulation (74,88–90,97), and its role in inducing *in vivo* repair (remodeling) and adaptation (4); these roles are briefly discussed below.

The effect of aging on the fatigue behavior has been addressed by Zioupos et al. (89) who reported higher fatigue lifetimes for femoral bone taken from a 27-year old as compared with a 56-year old donor (Fig. 14a). The same authors also showed that bovine femoral bone is stronger in tensile fatigue than red deer antler (Fig. 14b) (90). Data for bovine and human bone from a number of other studies are included in Fig. 14. Although confounding factors such as differences in test frequency, loading mode, and temperature make direct interpretation difficult, data from Swanson et al. (81) for human bone and from Carter and Caler (84) for bovine bone suggest that human bone is weaker than bovine bone in fatigue. However, it has recently been suggested that such differences may be age-related—most data for human bone, for obvious reasons, is from aged donors, and as such would be expected to have poorer mechanical properties (5). A definite effect of frequency on the *S*/*N* behavior exists, with higher frequencies giving higher fatigue-cycle lifetimes (83,96,106), as discussed below in the context of mechanistic aspects for bone fatigue. Loading mode and test geometry have also been reported to have an effect on fatigue lifetimes. Zero-compression loading generally gives only slightly higher lifetimes (10–15%) than zero-tension loading (106), although data from Pattin et al. (88) suggest a higher critical threshold exists for damage accumulation during fatigue under compressive loading (4000 $\mu\varepsilon$ vs. 2500 $\mu\varepsilon$). Vashishth et al. (95) reported a reduction in fatigue lifetimes when torsional loading was superimposed on tension-compression axial loading; similar results were seen for torsion as compared with compressive axial loading (99). With regards to test geometry, three-point bending has been claimed to induce less stiffness loss (reflective of fatigue damage) as compared with four-point bending (93); data in Ref. 89 further suggests that fatigue lifetimes in human bone are progressively decreased by testing in (four-point) bending, rotating cantilever, and zero-tension loading. Both latter studies presumably reflect that fatigue damage will accumulate more readily in test geometries with larger statistical "sampling" volumes. These reported results of the fatigue of bone are, on the whole, in line with the typical fatigue behavior displayed by most common engineering materials (105), although variations in variables such as temperature, donor age, and so on complicates comparisons between studies.

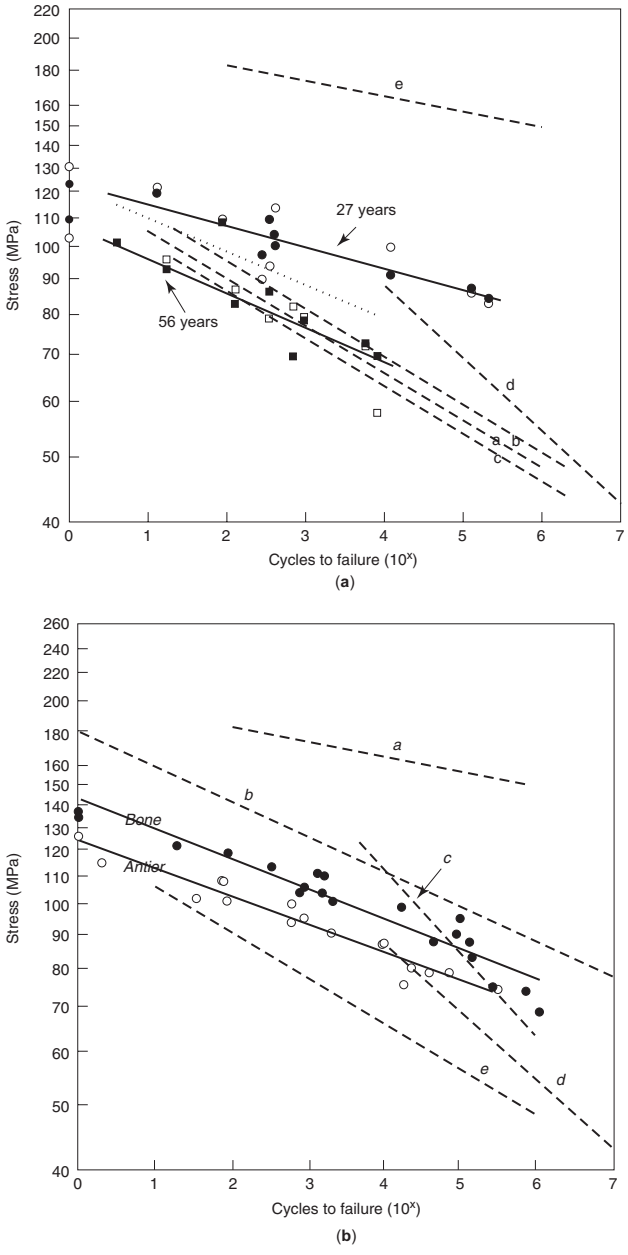

Figure 14. Fatigue stress-life *S*/*N* data for bone: (a) The effect of age in reducing the fatigue lifetimes is evident (open symbols- raw data, closed symbols- modulus-corrected data). Dotted lines (marked a–e) show data from other studies (see Ref. 89 for details), (b) The effect of species on fatigue lifetimes is shown. In addition to data for bovine femoral bone and red deer antler, dotted lines (marked a–e) show data from other studies: a,d,e- human, b,c- bovine (see Ref. 90 for details) [courtesy: Zioupos et al., (89,90)].

[1]Resulting *S*/*N* curves in certain materials, such as steels, can exhibit a plateau in the stress-life plot at $\sim 10^6$ cycles and beyond, which corresponds to a cyclic stress termed the *fatigue limit*, below which failure in principle does not occur (105). In the absence of a fatigue limit, a fatigue *endurance strength* is generally defined as the alternating stress to give a specific number of cycles to failure, typically 10^6 or 10^7 cycles (105).

Despite the plethora of fatigue data, mechanistically the role of fatigue loading in bone is still somewhat uncertain. Microdamage in bone was first reported over 40 years ago in the work of Frost (107), and a number of more recent studies have looked at methods of imaging such damage (108–110), how fatigue cycling can induce it (74,88–90,97), the loss is mechanical properties because of such damage (88), and the role of damage in triggering remodeling *in vivo* (4). Indeed, this aspect of fatigue in bone is one of the most studied; for further details, the interested reader is referred to the excellent review in Ref. 5.

One critical issue is whether fatigue damage is time- or cycle-dependent (or indeed both). One approach to address this issue has been to examine the role of test frequency on *S*/*N* behavior—a time-dependent mechanism is implied if the times-to-failure for different test frequencies are identical. Such studies, from Caler and Carter (106), Lafferty and Raju (83), and Zioupos et al. (96), suggest that tensile fatigue in bone can be time-dependent, because when plotted with respect to time, the effect of test frequency [0.002–2 Hz in (106) 30–125 Hz in (83), and 0.5–5 Hz in (96)] on the fatigue lifetimes is essentially eliminated (5,96). To explain these observations, Carter and Caler (111), and subsequently Taylor (5), have suggested that a transition exist in bone from a "creep" —dominated to a fatigue-dominated regime with decreasing stress levels. Although a classic creep mechanism may not actually contribute to this effect, it seems clear that the subcritical cracking behavior described above plays a role in this transition exists (100). However, because failure times in fatigue include both crack initiation and propagation stages, *S*/*N* results are not easy to interpret. Furthermore, in bone, where an inherent population of flaws/cracks typically exists, the crack initiation life may be less important. For this reason, many recent studies on the fatigue of bone have concentrated instead on the crack propagation life.

To analyze crack propagation lives, a fracture mechanics methodology, termed the *damage-tolerant* approach, may be used where the crack-propagation rate, *da*/*dN*, is assessed in terms of the range in stress-intensity factor, ΔK, defined as the difference between the stress intensity at the maximum and minimum of the loading cycle (Fig. 15) (100,104,112). Fatigue lives may then be determined from the number of cycles required for an incipient crack to grow subcritically to a critical size, as defined by fracture toughness, using information relating *da*/*dN* to ΔK (105). The first such characterization of fatigue-crack growth in bone, by Wright and Hayes (112), used longitudinally oriented bovine bone specimens to measure crack-growth rates for long cracks (i.e., cracks that are large as compared with the microstructural features of the underlying material) over growth rates of $da/dN \sim 7 \times 10^{-7}$ to $\sim 3 \times 10^{-4}$ m/cycle. These results were fitted to a simple Paris power-law formulation (113):

$$da/dN = C(\Delta K)^m, \tag{6}$$

where C and m (Paris exponent) are scaling constants; values of m were found to be between 2.8 to 5.1. Although Wright and Hayes' data did suggest some effect of cyclic frequency on crack-growth rates, their results were not conclusive. A subsequent study, by Gibeling et al. (104), measured a Paris exponent of $m \sim 10$ for transverse crack-

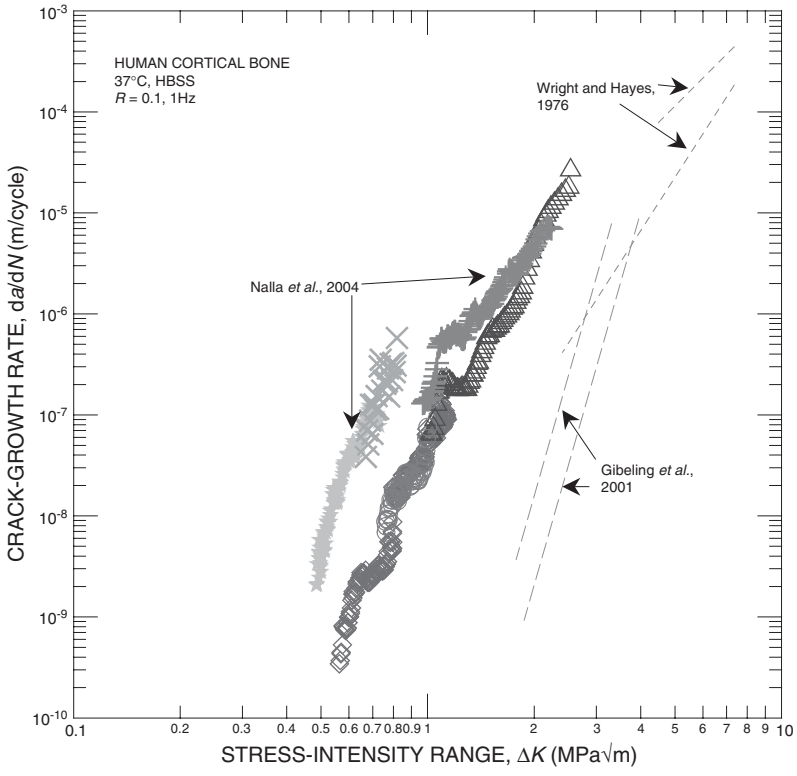

Figure 15. Variation in *in vitro* fatigue-crack growth rates, *da*/*dN*, as a function of the stress-intensity range, ΔK. Data shown as individual points are for crack growth in the longitudinal (proximal-distal) orientation in human humeral cortical bone (100). Also included (as dotted lines) are data from Wright and Hayes (112) for longitudinal crack growth in bovine bone and from Gibeling et al. (104) for transverse crack growth in equine bone.

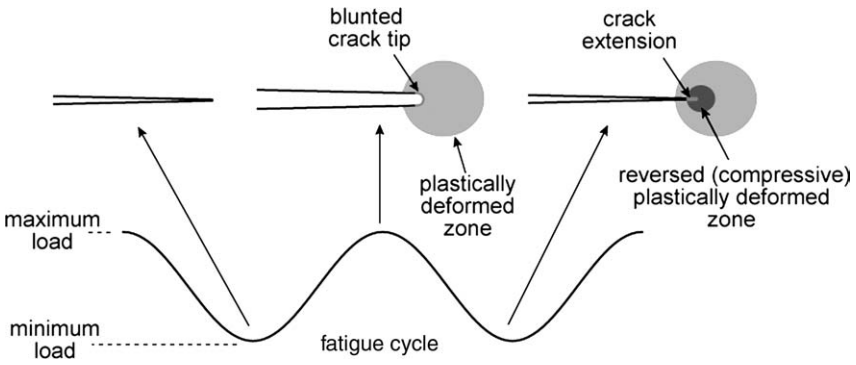

Figure 16. Schematic illustrating the alternating crack blunting and resharpening mechanism for fatigue crack growth in cortical bone. The crack is sharp at the beginning of the loading cycle, is blunted at the peak of the loading cycle, and is resharpened (and consequently extended) after unloading.

growth rates of $\sim 6 \times 10^{-10}$ to $\sim 1 \times 10^{-5}$ m/cycle in osteonal equine bone. For human bone, only one study has been reported to date; here, Nalla et al. (100) measured m values of $\sim$4.4–9.5 for longitudinal fatigue-crack growth rates over a wide range from $\sim 2 \times 10^{-10}$ to $\sim 3 \times 10^{-5}$ m/cycle in human cortical bone taken from the humerus. This work further showed a transition from predominantly time-dependent cracking at higher ΔK values to a true fatigue (cycle-dependent) mechanism at lower ΔK values, with this transition occurring at crack growth rates near 5×10^{-7} m/cycle. Although a specific mechanism for subcritical crack growth under *static* loading has not been proposed, the *cyclic* mechanism in bone has been reasoned to involve crack extension via alternating blunting and resharpening of the crack tip (100), not unlike what is seen in many ductile materials, such as metals and polymers (105). Figure 16 shows a schematic of this proposed mechanism.

Finally, extrinsic toughening is another factor that must be considered when assessing the fatigue behavior of cortical bone. Evidence for increasing crack growth resistance with crack extension has been observed in studies on surface cracks in cortical bone from human humeri and femera (94,102), and this effect has recently been associated with crack bridging (102). Bridges that form in the crack wake may sustain loads that reduce the local stress intensity range, ΔK, experienced at the crack tip, affecting the corresponding crack growth rates. As seen with the fracture toughness, this behavior leads to a crack size effect on the fatigue properties (i.e., the crack propagation resistance increases as the bridging zone develops). Another important factor that influences the growth microcracks in cortical bone is crack deflection because of cement lines, which in many cases causes microcracks to arrest (101,103) and may also be responsible for the formation of crack bridges as cracks imperfectly reconnect after deflecting around secondary osteons along the cement lines.

6. CONCLUDING REMARKS

Biological materials such as bone are complex structural materials with mechanical properties dictated by a hierarchical microstructure and an ability to (1) repair themselves and (2) adapt to changing environmental and loading conditions. Accordingly, it is not surprising that the problem of understanding the fracture of bone is equally complex. By addressing the intrinsic and extrinsic toughening mechanisms, clearer ideas have emerged of late as to the nature of the fracture resistance of bone. However, a mechanistic understanding of the increased *in vivo* fracture risk associated with factors such as aging, disease, or cyclic loading, and how they relate to fracture properties measured *in vitro*, is still relatively limited. The ultimate goal is to determine the specific mechanisms involved in the fracture and fatigue of bone, and to discover how these mechanisms relate to features within the hierarchical microstructure of bone. Such an understanding will greatly aid the development of treatments or prevention methods for conditions such as bone fragility and osteoporosis, which specifically target the key microstructural aspects that provide the fracture resistance of bone. As noted above, progress has been made with regard to a mechanistic understanding of bone fracture, but the degree of understanding is still limited. Consequently, the authors believe that bone fracture will continue to remain an area of intense research for the foreseeable future.

Acknowledgments

This work was supported in part by the National Institutes of Health under Grant No. 5R01 DE015633 (for RKN), and by the Director, Office of Science, Office of Basic Energy Science, Division of Materials Sciences and Engineering of the Department of Energy under Contract No. DE-AC02-05CH11231 (for JJK and ROR).

BIBLIOGRAPHY

1. H. H. Jones, J. D. Priest, W. C. Hayes, C. C. Tichenor, and D. A. Nagel, Human hypertrophy in response to exercise. *J. Bone Joint Surg*. 1977; **59A**:204–208.
2. D. B. Burr, R. B. Martin, M. Schaffler, and E. L. Radin, Bone remodeling in response to *in vivo* fatigue microdamage. *J. Biomech*. 1985; **18**:189–200.
3. S. Mori and D. B. Burr, Increased intracortical remodeling following fatigue damage. *Bone* 1993; **14**:103–109.
4. T. C. Lee, A. Staines, and D. Taylor, Bone adaptation to load: microdamage as a stimulus for bone remodelling. *J. Anat*. 2002; **201**:437–446.
5. D. Taylor, Failure processes in hard and soft tissues. In: I. Milne, R. O. Ritchie, and B. Karihaloo, eds., *Comprehensive*

Structural Integrity: Fracture of Materials from Nano to Macro, vol. 9. Oxford, UK: Elsevier Science, 2003. pp. 35–95.

6. R. Heaney, Is the paradigm shifting? *Bone* 2003; **33**(4):457–465.
7. B. L. Riggs, L. J. Melton III, and W. M. O'Fallon, Drug therapy for vertebral fractures in osteoporosis: evidence that decreases in bone turnover and increases in bone mass both determine antifracture efficacy. *Bone* 1996; **18**(3):197S–201S.
8. J. D. Currey, Changes in impact energy absorption with age. *J. Biomech*. 1979; **12**:459–469.
9. W. Bonfield, J. C. Behiri, and C. Charalamides, Orientation and age-related dependence of the fracture toughness of cortical bone. In: S. M. Perren and E. Schneider, eds., *Biomechanics: Current Interdisiplinary Research*. Dodrecht, The Netherlands: Martinum Nijhoff Publishers, 1985.
10. C. U. Brown and T. L. Norman, Fracture toughness of human cortical bone from the proximal femur. *Adv. Bioeng*. 1995; **31**:121–122.
11. J. D. Currey, K. Brear, and P. Zioupos, The effects of aging and changes in mineral content in degrading the toughness of human femora. *J. Biomech*. 1996; **29**(2):257–260.
12. Y. N. Yeni, C. U. Brown, Z. Wang, and T. L. Norman, The influence of bone morphology on fracture toughness of the human femur and tibia. *Bone* 1997; **21**(5):453–459.
13. X. D. Wang, N. S. Masilamani, J. D. Mabrey, M. E. Alder, and C. M. Agrawal, Changes in the fracture toughness of bone may not be reflected by its mineral density, porosity, and tensile properties. *Bone* 1998; **23**(1):67–72.
14. J. –Y. Rho, L. Kuhn-Spearing, and P. Zioupos, Mechanical properties and the hierarchical structure of bone. *Med. Eng. Phys*. 1998; **20**:92–102.
15. Y. N. Yeni, C. U. Brown, and T. L. Norman, Influence of bone composition and apparent density on fracture toughness of the human femur and tibia. *Bone* 1998; **22**(1):79–84.
16. S. Weiner and H. D. Wagner, The material bone: structure-mechanical function relations. *Annu. Rev. Mater. Sci*. 1998; **28**:271–298.
17. P. Zioupos and J. D. Currey, Changes in the stiffness, strength, and toughness of human cortical bone with age. *Bone* 1998; **22**:57–66.
18. P. Braidotti, E. Bemporad, T. D'Alessio, S. A. Sciuto, and L. Stagni, Tensile experiments and SEM fractography on bovine subchondral bone. *J. Biomech*. 2000; **33**(9):1153–1157.
19. C. U. Brown, Y. N. Yeni, and T. L. Norman, Fracture toughness is dependent on bone location—A study of the femoral neck, femoral shaft, and the tibial shaft. *J. Biomed. Mater. Res*. 2000; **49**:380–389.
20. G. C. Reilly and J. D. Currey, The effects of damage and microcracking on the impact strength of bone. *J. Biomech*. 2000; **33**:337–343.
21. D. Vashishth, K. E. Tanner, and W. Bonfield, Contribution, development and morphology of microcracking in cortical bone during crack propagation. *J. Biomech*. 2000; **33**:1169–1174.
22. Y. N. Yeni and T. L. Norman, Fracture toughness of human femoral neck: effect of microstructure, composition, and age. *Bone* 2000; **26**(5):499–504.
23. Y. N. Yeni and T. L. Norman, Calculation of porosity and osteonal cement line effects on the effective fracture toughness of cortical bone in longitudinal crack growth. *J. Biomed. Mater. Res*. 2000; **51**:504–509.
24. G. P. Parsamian and T. L. Norman, Diffuse damage accumulation in the fracture process zone of human cortical bone specimens and its influence on fracture toughness. *J. Mater. Sci. Mater. Med*. 2001; **12**:779–783.
25. X. Wang, R. Bank, J. Tekoppele, and C. Agrawal, The role of collagen in determining bone mechanical properties. *J. Orthop. Res*. 2001; **19**:1021–1026.
26. X. Wang, X. Shen, X. Li, and C. M. Agrawal, Age-related changes in the collagen network and toughness of bone. *Bone* 2002;**31**(1):1–7.
27. L. P. Hiller, S. M. Stover, V. A. Gibson, J. C. Gibeling, C. S. Prater, S. J. Hazelwood, et al., Osteon pullout in the equine third metacarpal bone: effects of ex vivo fatigue. *J. Orthop. Res*. 2003; **21**(3):481–488.
28. D. Vashishth, K. E. Tanner, and W. Bonfield, Experimental validation of a microcracking-based toughening mechanism for cortical bone. *J. Biomech*. 2003; **36**:121–124.
29. R. K. Nalla, J. H. Kinney, and R. O. Ritchie, Mechanistic fracture criteria for the failure of human cortical bone. *Nature Mater*. 2003; **2**(3): 164–168.
30. J. B. Phelps, G. B. Hubbard, X. Wang, and C. M. Agrawal, Microstructural heterogeneity and the fracture toughness of bone. *J. Biomed. Mater. Res*. 2000; **51**(4):735–741.
31. J. D. Currey, 'Osteons' in biomechanical literature. *J. Biomech*. 1982; **15**:717.
32. P. Lucksanambool, W. A. J. Higgs, R. J. E. D. Higgs, and M. W. Swain, Fracture toughness of bovine bone: influence of orientation and storage media. *Biomaterials* 2001; **22**:3127–3132.
33. J. F. Knott, *Fundamentals of Fracture Mechanics*. London: Butterworth & Co, 1976.
34. W. Bonfield, M. D. Grynpas, and R. J. Young, Crack velocity and the fracture of bone. *J. Biomech*. 1978; **11**:473–479.
35. J. C. Behiri and W. Bonfield, Crack velocity dependence of longitudinal fracture in bone. *J. Mater. Sci*. 1980; **15**:1841–1849.
36. T. M. Wright and W. C. Hayes, Fracture mechanics parameters for compact bone—Effects of density and specimen thickness. *J. Biomech*. 1977; **10**:419–430.
37. J. C. Behiri and W. Bonfield, Fracture mechanics of bone—The effects of density, specimen thickness, and crack velocity on longitudinal fracture. *J. Biomech*. 1984; **17**(1):25–34.
38. T. L. Norman, D. Vashishth, and D. B. Burr, Fracture toughness of human bone under tension. *Biomech*. 1995; **28**(3):309–320.
39. J. C. Behiri and W. Bonfield, Orientation dependence of fhe fracture mechanics of cortical bone. *J. Biomech*. 1989; **22**(8/9):863–872.
40. D. M. Robertson, D. Robertson, and C. R. Barrett, Fracture toughness, critical crack length and plastic zone size in bone. *J. Biomech*. 1978; **11**:359–364.
41. ASTM E399-90 (Reapproved 1997). In: *Annual Book of ASTM Standards, Vol. 03.01*: *Metals-Mechanical Testing*; *Elevated and Low-Temperature Tests*; *Metallography.* West Conshohocken, PA: ASTM, 2002.
42. J. D. Currey, Mechanical properties of vertebrate hard tissues. *Proc. Instn. Mech. Engrs*. 1998; **212H**:399–412.
43. T. L. Norman, S. V. Nivargikar, and D. B. Burr, Resistance to crack growth in human cortical bone is greater in shear than in tension. *J. Biomech*. 1996; **29**(8):1023–1031.
44. Z. Feng, J. Rho, S. Han, and I. Ziv, Orientation and loading condition dependence of fracture toughness in cortical bone. *Mater. Sci. Eng. C*. 2000; **C11**:41–46.

45. P. Zioupos, J. D. Currey, and A. J. Hamer, The role of collagen in the declining mechanical properties of aging human cortical bone. *J. Biomed. Mater. Res*. 1999; **2**:108–116.
46. O. Akkus, F. Adar, and M. B. Schaffler, Age-related changes in physicochemical properties of mineral crystals are related to impaired mechanical function of cortical bone. *Bone* 2004; **34**(3):443–453.
47. A. H. Burstein, D. T. Reilly, and M. Martens, Aging of bone tissue: mechanical properties. *J. Bone Joint Surg. Am*. 1976; **58**(1):82–86.
48. E. Seeman, The structural basis of bone fragility in men. *Bone* 1999; **25**(1):143–147.
49. D. D. Moyle and R. W. Bowden, Fracture of human femeral bone. *J. Biomech*. 1984; **17**(3):203–213.
50. G. Corondan and W. L. Haworth, A fractographic study of human long bone. *J. Biomech*. 1986; **19**(3):207–218.
51. T. L. Norman and Z. Wang, Microdamage of human cortical bone: Incidence and morphology in long bones. *Bone* 1997; **20**(4):375–379.
52. D. B. Burr, M. B. Schaffler, and R. G. Frederickson, Composition of the cement line and its possible mechanical role as a local interface in compact bone. *J. Biomech*. 1988; **21**(11):939–945.
53. R. K. Nalla, J. J. Kruzic, J. H. Kinney, and R. O. Ritchie, Mechanistic aspects of fracture and R-curve behavior of human cortical bone. *Biomaterials* 2005; **26**(2):217–231.
54. R. B. Martin and D. B. Burr, A hypothetical mechanism for the stimulation of oteonal remodeling by fatigue damage. *J. Biomech*. 1982; **15**:137–139.
55. X. Wang, X. Li, R. A. Bank, and C. M. Agrawal, Effects of collagen unwinding and cleavage on the mechanical integrity of the collagen network in bone. *Calcif. Tissue Int*. 2002; **71**(2):186–192.
56. D. H. Pashley, K. A. Agee, R. M. Carvalho, K. –W. Lee, F. R. Tay, and T. E. Callison, Effects of water and water-free polar solvents on the tensile properties of demineralized dentin. *Dent Mater*. 2003; **19**:347–352.
57. B. R. Lawn, Physics of fracture. *J. Am. Ceram. Soc*. 1983; **66**(2):83–91.
58. A. G. Evans, Perspective on the development of high toughness ceramics. *J. Am. Ceramic. Soc*. 1990; **73**:187–206.
59. R. O. Ritchie, Mechanisms of fatigue crack propagation in metals, ceramics and composites: role of crack tip shielding. *Mater. Sci. Eng*. 1988; **A103**:15–28.
60. R. O. Ritchie, Mechanisms of fatigue-crack propagation in ductile and brittle solids. *Int. J. Fract*. 1999; **100**(1):55–83.
61. G. Pezzotti and S. Sakakura, Study of the toughening mechanisms in bone and biomimetic hydroxyapatite materials using Raman microprobe spectroscopy. *J. Biomed. Mater. Res*. 2003; **65A**(2):229–236.
62. R. K. Nalla, J. J. Kruzic, and R. O. Ritchie, On the origin of the toughness of mineralized tissue: microcracking or crack bridging? *Bone* 2004; **34**(5):790–798.
63. D. Vashishth, Rising crack-growth-resistance behavior in cortical bone: implication for toughness measurements. *J. Biomech*. 2004; **37**(6):943–946.
64. D. Vashishth, J. C. Behiri, and W. Bonfield, Crack growth resistance in cortical bone: concept of microcrack toughening. *J. Biomech*. 1997; **30**(8):763–769.
65. C. L. Malik, S. M. Stover, R. B. Martin, and J. C. Gibeling, Equine cortical bone exhibits rising R-curve fracture mechanics. *J. Biomech*. 2003; **36**:191–198.
66. R. K. Nalla, J. J. Kruzic, J. H. Kinney, and R. O. Ritchie, Effect of aging on the toughness of human cortical bone: evaluation by R-curves. *Bone* 2004; **35**(6):1240–1246.
67. T. M. Keaveny, E. F. Wachtel, C. M. Ford, and W. C. Hayes, Differences between the tensile and compressive strengths of bovine tibial trabecular bone depend on modulus. *J. Biomech*. 1994; **27**(9):1137–1146.
68. C. M. Ford and T. M. Keaveny, The dependence of shear failure properties of trabecular bone on apparent density and trabecular orientation. *J. Biomech*. 1996; **29**(10):1309–1317.
69. O. C. Yeh and T. M. Keaveny, Relative roles of microdamage and microfracture in the mechanical behavior of trabecular bone. *J. Orthop. Res*. 2001; **19**(6):1001–1007.
70. R. K. Nalla, J. J. Kruzic, J. H. Kinney, M. Balooch, J. W. Ager III, and R. O. Ritchie, Role of microstructure in the aging-related deterioration of the toughness of human cortical bone. *Mater. Sci. Eng. C*. 2006; **26**(2).
71. X. Wang, X. Li, R. A. Bank, and C. M. Agrawal, Effect of collagen unwinding and cleavage on the mechanical integrity of the collagen network in bone. *Calcif. Tissue Int*. 2002; **71**:186–192.
72. A. G. Evans and K. T. Faber, Crack-growth resistance of microcracking brittle materials. *J. Am. Ceram. Soc*. 1984; **67**(4):255–260.
73. J. W. Hutchinson, Crack tip shielding by micro-cracking in brittle solids. *Acta Metall*. 1987; **35**(7):1605–1619.
74. Y. N. Yeni and D. P. Fyhrie. Fatigue damage-fracture mechanics interaction in cortical bone. *Bone* 2002; **30**(3):509–514.
75. L. S. Sigl, Microcrack toughening in brittle materials containing weak and strong interfaces. *Acta Mater*. 1996; **44**(9):3599–3609.
76. Y. N. Yeni and D. P. Fyhrie, A rate-dependent microcrack-bridging model that can explain the strain rate dependency of cortical bone apparent yield strength. *J. Biomech*. 2003; **36**(9): 1343–1353.
77. J. Iwamoto and T. Takeda, Stress fractures in athletes: review of 196 cases. *J. Orthop. Sci*. 2003; **8**(3):273–278.
78. D. B. Burr, Bone exercise and stress fractures. *Exerc. Sport Sci. Rev.* 1997; **25**:171–194.
79. K. O. Meurman and S. Elfving, Stress fracture in soldiers: a multifocal bone disorder. A comparative radiological and scintigraphic study. *Radiology* 1980; **134**(2):483–487.
80. F. G. Evans and M. Lebow, Strength of human compact bone under repetitive loading. *J. Appl. Physiol*. 1957; **10**(1):127–130.
81. S. A. Swanson, M. A. Freeman, and W. H. Day, The fatigue properties of human cortical bone. *Med. Biol. Eng*. 1971; **9**(1):23–32.
82. D. R. Carter and W. C. Hayes, Fatigue life of compact bone—I. Effects of stress amplitude, temperature and density. *J. Biomech*. 1976; **9**(1):27–34.
83. J. F. Lafferty and P. V. V. Raju, The effect of stress frequency on the fatigue strength of cortical bone. *J. Biomech. Eng*. 1979; **101**:112–113.
84. D. R. Carter and W. E. Caler, Cycle-dependent and time-dependent bone fracture with repeated loading. *J. Biomech. Eng*. 1983; **105**(2):166–170.
85. W. E. Caler and D. R. Carter, Bone creep-fatigue damage accumulation. *J. Biomech*. 1989; **22**(6–7):625–635.

86. M. B. Schaffler, E. L. Radin, and D. B. Burr, Mechanical and morphological effects of strain rate on fatigue of compact bone. *Bone* 1989; **10**(3):207–214.

87. T. M. Boyce, D. P. Fyhrie, F. R. Brodie, and M. B. Schaffler, Residual mechanical properties of human cortical bone following fatigue loading. In: 20th Annual Meeting of the American Society of Biomechanics, Atlanta, Georgia, 1996.

88. C. A. Pattin, W. E. Caler, and D. R. Carter, Cyclic mechanical property degradation during fatigue loading of cortical bone. *J. Biomech*. 1996; **29**(1):69–79.

89. P. Zioupos, X. T. Wang, and J. D. Currey, The accumulation of fatigue microdamage in human cortical bone of two different ages in vitro. *Clin. Biomech*. 1996; **11**:7.

90. P. Zioupos, X. T. Wang, and J. D. Currey, Experimental and theoretical quantification of the development of damage in fatigue tests of bone and antler. *J. Biomech*. 1996; **29**(8):989–1002.

91. R. B. Martin, V. A. Gibson, S. M. Stover, J. C. Gibeling, and L. V. Griffin, Residual strength of equine bone is not reduced by intense fatigue loading: Implications for stress fracture. *J. Biomech*. 1997; **30**(2):109–114.

92. D. Taylor, Microcrack growth parameters for compact bone deduced from stiffness variations. *J. Biomech*. 1998; **31**:587–592.

93. L. V. Griffin, J. C. Gibeling, R. B. Martin, V. A. Gibson, and S. M. Stover, The effects of testing methods on the flexural fatigue life of human cortical bone. *J. Biomech*. 1999; **32**(1):105–109.

94. O. Akkus and C. M. Rimnac, Cortical bone tissue resists fatigue fracture by deceleration and arrest of microcrack growth. *J. Biomech*. 2001; **34**(6):757–764.

95. D. Vashishth, K. E. Tanner, and W. Bonfield, Fatigue of cortical bone under combined axial-torsional loading. *J. Orthop. Res*. 2001; **19**(3):414–420.

96. P. Zioupos, J. D. Currey, and A. Casinos, Tensile fatigue in bone: are cycles-, or time to failure, or both, important? *J. Theor. Biol*. 2001; **210**(3):389–399.

97. C. Fleck and D. Eifler, Deformation behaviour and damage accumulation of cortical bone specimens from the equine tibia under cyclic loading. *J. Biomech*. 2003; **36**(2):179–189.

98. R. B. Martin, Fatigue damage, remodeling, and the minimization of skeletal weight. *J. Theor. Biol*. 2003; **220**(2):271–276.

99. D. Taylor, P. O'Reilly, L. Vallet, and T. C. Lee, The fatigue strength of compact bone in torsion. *J. Biomech*. 2003; **36**(8):1103–1109.

100. R. K. Nalla J. J. Kruzic, J. H. Kinney, and R. O. Ritchie, Aspects of in vitro fatigue in human cortical bone: time and cycle dependent crack growth. *Biomaterials* 2005; **26**(14):2183–2195.

101. F. J. O'Brien, D. Taylor, and T. C. Lee, Microcrack accumulation at different intervals during fatigue testing in compact bone. *J. Biomech*. 2003; **36**(7):973–980.

102. J. J. Kruzic, J. A. Scott, R. K. Nalla, and R. O. Ritchie, Propagation of surface fatigue cracks in human cortical bone. *J. Biomech*. 2006; **39**(5).

103. F. J. O'Brien, D. Taylor, and T. Clive Lee, The effect of bone microstructure on the initiation and growth of microcracks. *J. Orthop. Res*. 2005; **23**(2):475–480.

104. J. C. Gibeling, D. R. Shelton, and C. L. Malik. Application of fracture mechanics to the study of crack propagation in bone. In: H. Rack, D. Lesuer, and E. Taleff, eds., *Structural Biomaterials for the 21st Century*. Warrendale, PA: TMS, 2001, pp. 239–254.

105. S. Suresh, *Fatigue of Materials*. 2nd ed. Cambridge, UK: Cambridge University Press, 1998.

106. W. E. Caler and D. R. Carter, Bone-creep fatigue damage accumulation. *J. Biomech*. 1989; **22**:625–635.

107. H. M. Frost, Presence of microscopic cracks *in vivo* in bone. *Henry Ford Hospital Med. Bull*. 1960; **8**:25–35

108. T. C. Lee, E. R. Myers, and W. C. Hayes, Fluorescence-aided detection of microdamage in compact bone. *J. Anat*. 1998; **193**(2):179–184.

109. T. C. Lee, T. L. Arthur, L. J. Gibson, and W. C. Hayes, Sequential labelling of microdamage in bone using chelating agents. *J. Orthop. Res*. 2000; **18**(2):322–325.

110. T. C. Lee, S. Mohsin, D. Taylor, R. Parkesh, T. Gunnlaugsson, F. J. O'Brien, et al., Detecting microdamage in bone. *J. Anat*. 2003; **203**(2):161–172.

111. D. R. Carter and W. E. Caler, A cumulative damage model for bone fracture. *J. Orthop. Res*. 1985; **3**:84–90.

112. T. Wright and W. Hayes, The fracture mechanics of fatigue crack propagation in compact bone. *Biomed. Mater. Res. Symn. J. Biomed. Mater. Res*. 1976; **7**(10):637–648.

113. P. C. Paris, M. P. Gomez, and W. P. Anderson, A rational analytic theory of fatigue. *Trend Eng*. 1961; **13**:9–14.